Electronic Supplementary Information

Electrical Control of Biexciton Auger Recombination in Single CdSe/CdS Nanocrystals

Ying Tang,[a] Qilin Qin,[a] Hongyu Yang,[b] Shengnan Feng,[a] Chunfeng Zhang,[a] Jiayu Zhang,*[b] Min Xiao,[ac] and Xiaoyong Wang*[a]

[a.] *National Laboratory of Solid State Microstructures, School of Physics, and Collaborative Innovation Center of Advanced Microstructures, Nanjing University, Nanjing 210093, China*

[b.] *Advanced Photonics Center, School of Electronic Science and Engineering, Southeast University, Nanjing 210096, China*

[c.] *Department of Physics, University of Arkansas, Fayetteville, Arkansas 72701, USA*

**Correspondence to J.Z. (jyzhang@seu.edu.cn) or X.W. (wxiaoyong@nju.edu.cn)*

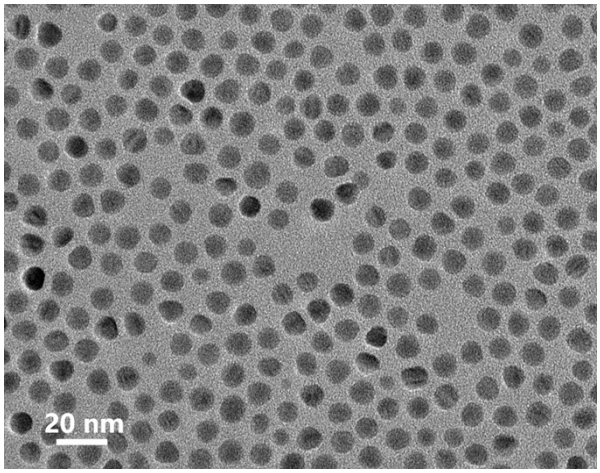

Fig. S1 Transmission electron microscopy image of CdSe/CdS *g*NCs.

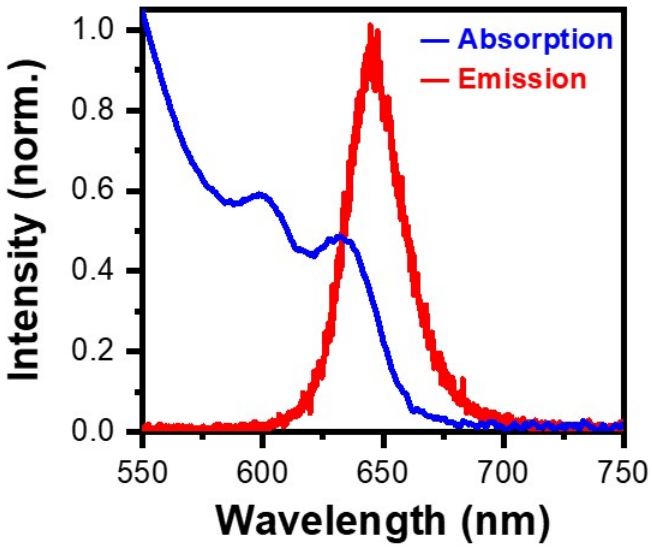

Fig. S2 Solution absorption and emission spectra of CdSe/CdS *g*NCs.

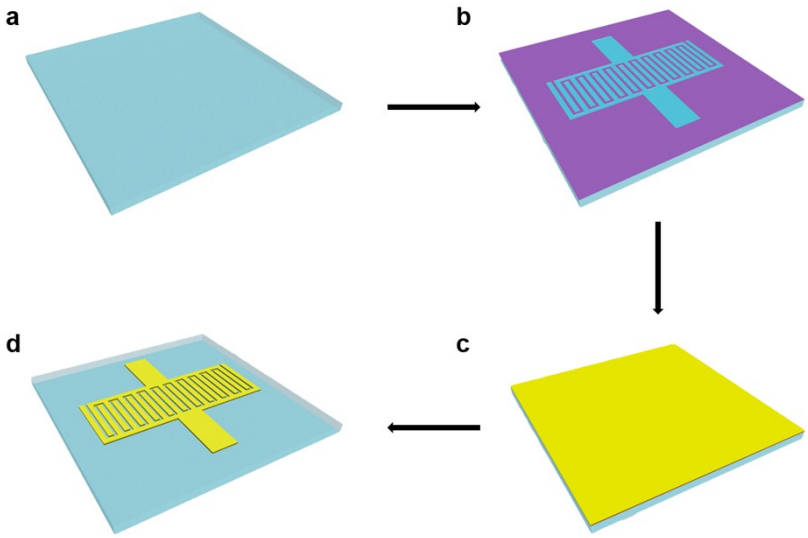

Fig. S3 Fabrication of electrodes. **(a)** A clean glass substrate was first prepared. **(b)** The substrate was next spin-coated with the photoresist, on top of which an interdigitated pattern was printed by extreme ultraviolet (EUV) lithography using a photomask. **(c)** The Au and Cr layers with the respective thicknesses of 80 and 5 nm were then deposited by the physical vapor deposition (PVD) system. **(d)** Finally, the substrate was soaked in acetone and ultrasonically cleaned for about 10 min to lift off the photoresist. In the as-fabricated sample, each electrode had a width of 10 µm and the two nearby electrodes were spatially separated by 5 µm.

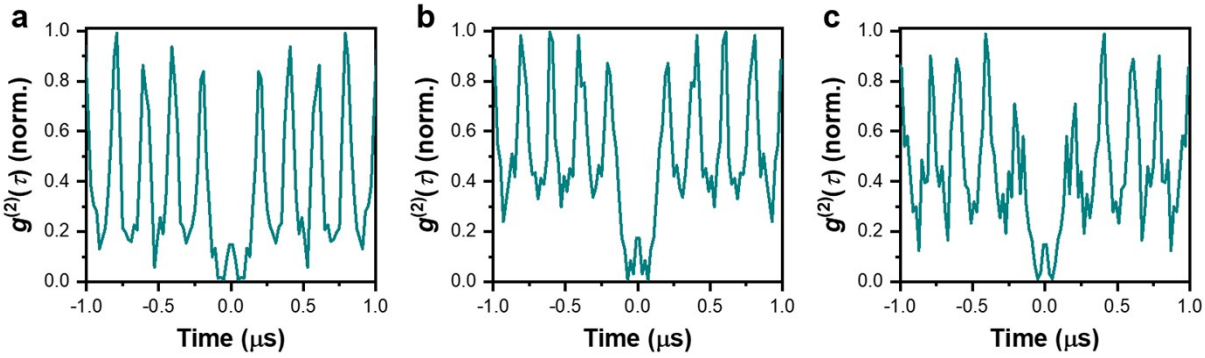

Fig. S4 Second-order photon correlation curves measured at <*N*> = ~0.1 for three single CdSe/CdS *g*NCs with the $g^{(2)}(0)$ values of **(a)** ~0.145, **(b)** ~0.160 and **(c)** ~0.149, respectively.

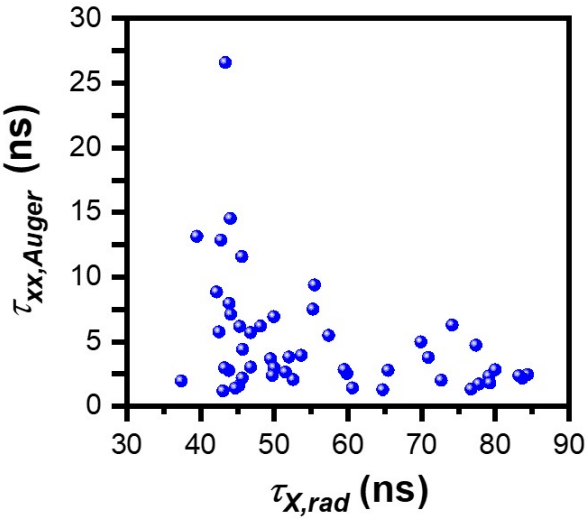

Fig. S5 The biexciton Auger lifetime $\tau_{XX,Auger}$ plotted as a function of the single-exciton radiative lifetime $\tau_{X,\,rad}$ for ~50 single CdSe/CdS *g*NCs excited at $< N >$ = ~0.5 without the electric field.

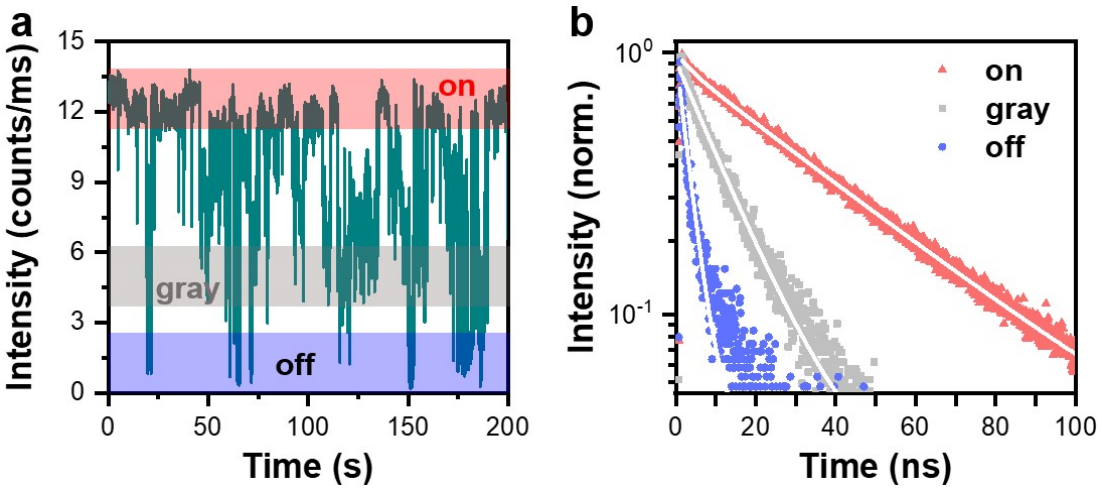

Fig. S6 (a) PL intensity time trace measured with a binning time of 10 ms for a single CdSe/CdS *g*NC excited at $< N >$ = ~0.5, where the "on", "gray" and "off" states are marked by the red, gray and blue shadings, respectively. **(b)** PL decay curves extracted from (a) for the "on", "gray" and "off" states, respectively. The PL decay curve of "on" state is fitted by a bi-exponential function with the fast and slow lifetimes of ~3.5 and ~36.8 ns, respectively. The PL decay curves of "gray" and "off" states are both fitted by the single-exponential functions with the respective lifetimes of ~11.8 and ~3.2 ns, respectively.

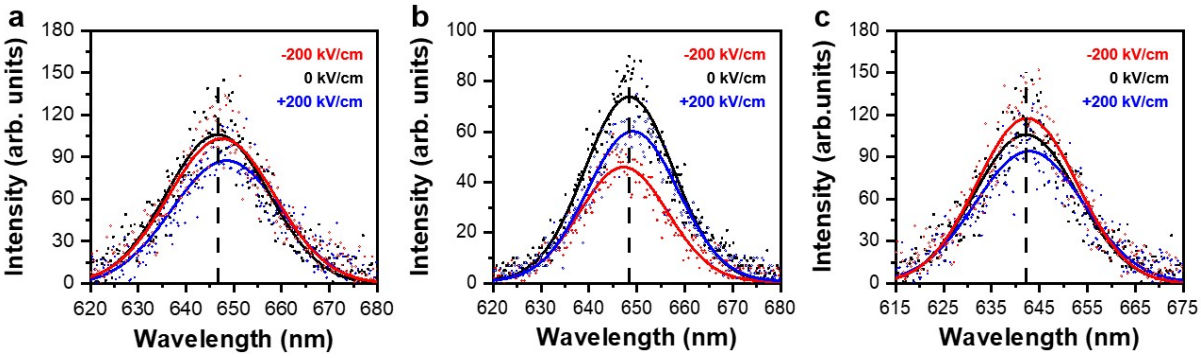

Fig. S7 (a) PL spectra measured at $< N >$ = ~0.1 for a single CdSe/CdS *g*NC, showing a red shift when the electric field of either 200 or -200 kV/cm is applied. **(b)** PL spectra measured at $< N >$ = ~0.1 for a single CdSe/CdS *g*NC, showing a red (blue) shift when the electric field of 200 (-200) kV/cm is applied. **(c)** PL spectra measured at $< N >$ = ~0.1 for a single CdSe/CdS *g*NC, showing no obvious shift in the PL peak when the electric field of either 200 or -200 kV/cm is applied. In (a)-(c), the black dashed lines mark the peak positions of the zero-field PL spectra.

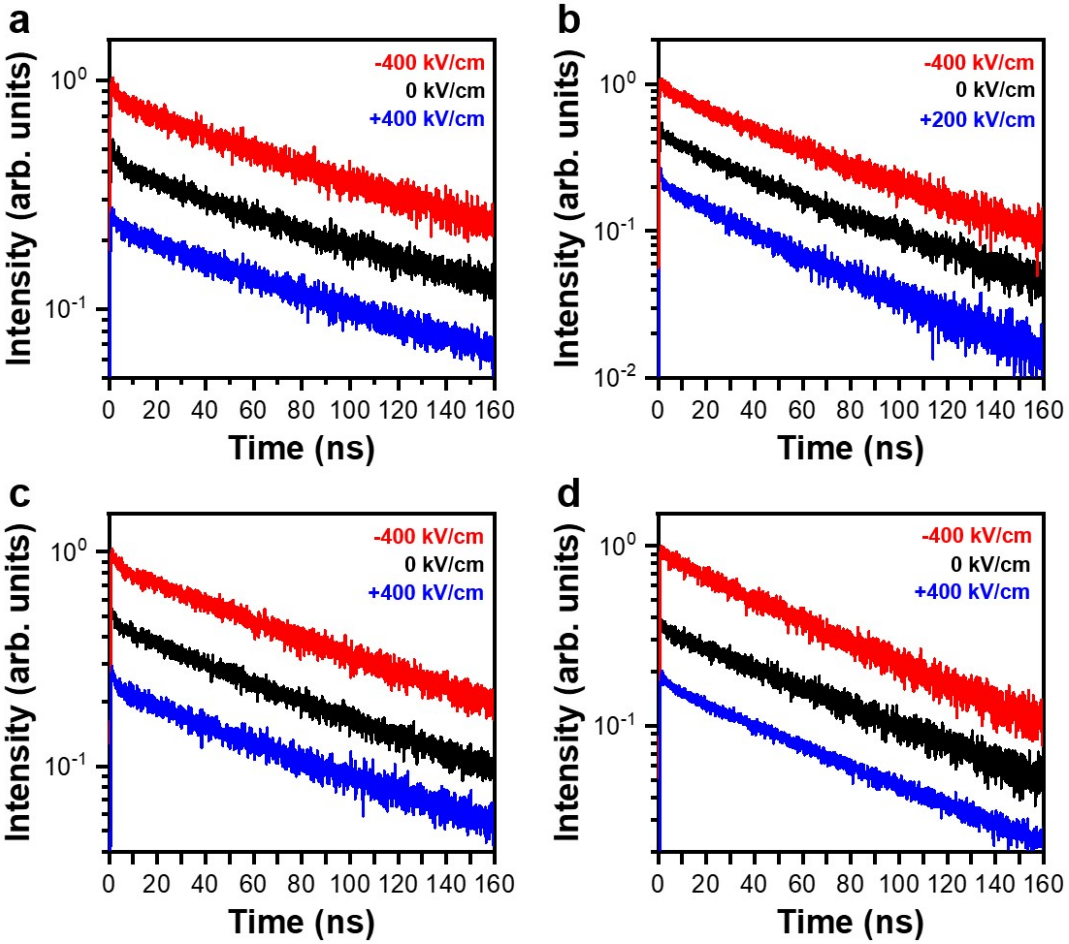

Fig. S8 (a) PL decay curves measured for a single CdSe/CdS *g*NC from the first type at the electric fields of -400, 0 and 400 kV/cm, respectively. **(b)** PL decay curves measured for a single CdSe/CdS *g*NC from the second type at the electric fields of -400, 0 and 200 kV/cm, respectively. **(c)** PL decay curves measured for a single CdSe/CdS *g*NC from the third type at the electric fields of -400, 0 and 400 kV/cm, respectively. **(d)** PL decay curves measured for a single CdSe/CdS *g*NC from the fourth type at the electric fields of -400, 0 and 400 kV/cm, respectively. In (a)-(d), the three PL decay curves are offset to each other for clarity.

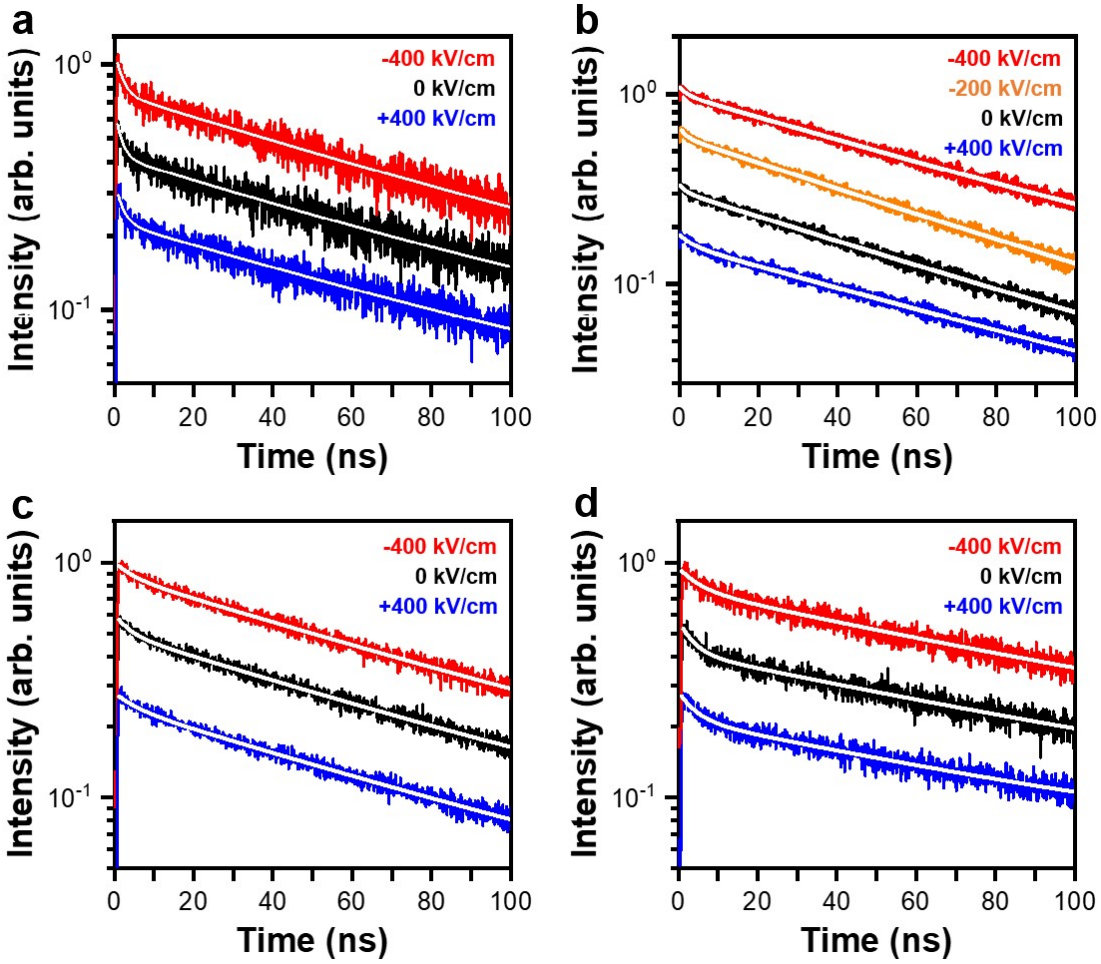

Fig. S9 (a) PL decay curves measured at $< N >$ = ~0.5 for a single CdSe/CdS *g*NC from the first type and each fitted by the solid line using a bi-exponential function. At 0 kV/cm, the obtained $\tau_{X,\,rad}$, $\tau_{XX,total}$ and $\tau_{XX,Auger}$ values are ~77.7, ~1.6 and ~1.7 ns, respectively. At -400 kV/cm, the obtained $\tau_{X,\,rad}$, $\tau_{XX,total}$ and $\tau_{XX,Auger}$ values are ~83.0, ~1.9 and ~2.1 ns, respectively. At 400 kV/cm, the obtained $\tau_{X,\,rad}$, $\tau_{XX,total}$ and $\tau_{XX,Auger}$ values are ~82.2, ~1.9 and ~2.1 ns, respectively. **(b)** PL decay curves measured at $< N >$ = ~0.5 for a single CdSe/CdS *g*NC from the second type and each fitted by the solid line using a bi-exponential function. At 0 kV/cm, the obtained $\tau_{X,\,rad}$, $\tau_{XX,total}$ and $\tau_{XX,Auger}$ values are ~64.2, ~1.8 and ~2.1 ns, respectively. At -400 kV/cm, the obtained $\tau_{X,\,rad}$, $\tau_{XX,total}$ and $\tau_{XX,Auger}$ values are ~69.9, ~2.2 and ~2.5 ns, respectively. At -200 kV/cm, the obtained $\tau_{X,\,rad}$, $\tau_{XX,total}$ and $\tau_{XX,Auger}$ values are ~61.6, ~1.6 and ~1.8 ns, respectively. At 400 kV/cm, the obtained $\tau_{X,\,rad}$, $\tau_{XX,total}$ and $\tau_{XX,Auger}$ values are ~72.0, ~3.3 and ~4.0 ns, respectively. The PL peak is blue-shifted at -200 kV/cm and red-shifted at ±400 kV/cm, as compared to the one measured at 0 kV/cm. **(c)** PL decay curves

measured at $< N >$ = ~0.5 for a single CdSe/CdS *g*NC from the third type and each fitted by the solid line using a bi-exponential function. At 0 kV/cm, the obtained $\tau_{X,\,rad}$, $\tau_{XX,total}$ and $\tau_{XX,Auger}$ values are ~77.7, ~3.6 and ~4.4 ns, respectively. At -400 kV/cm, the obtained $\tau_{X,\,rad}$, $\tau_{XX,total}$ and $\tau_{XX,Auger}$ values are ~80.0, ~4.5 and ~5.9 ns, respectively. At 400 kV/cm, the obtained $\tau_{X,\,rad}$, $\tau_{XX,total}$ and $\tau_{XX,Auger}$ values are ~78.9, ~5.3 and ~7.3 ns, respectively. **(d)** PL decay curves measured at $< N >$ = ~0.5 for a single CdSe/CdS *g*NC from the fourth type and each fitted by the solid line using a bi-exponential function. At 0 kV/cm, the obtained $\tau_{X,\,rad}$, $\tau_{XX,total}$ and $\tau_{XX,Auger}$ values are ~107.4, ~3.7 and ~4.3 ns, respectively. At -400 kV/cm, the obtained $\tau_{X,\,rad}$, $\tau_{XX,total}$ and $\tau_{XX,Auger}$ values are ~103.6, ~5.2 and ~6.5 ns, respectively. At 400 kV/cm, the obtained $\tau_{X,\,rad}$, $\tau_{XX,total}$ and $\tau_{XX,Auger}$ values are ~101.0, ~4.4 and ~5.3 ns, respectively. In (a)-(d), the three or four PL decay curves are offset to each other for clarity.

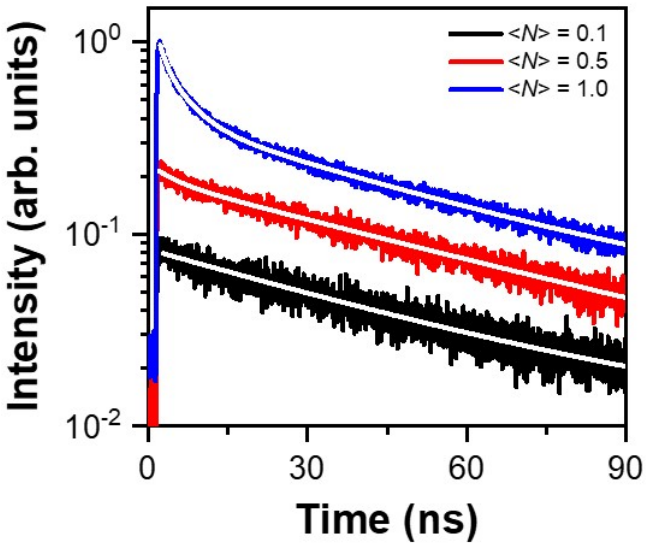

Fig. S10 PL decay curves measured for a single CdSe/CdS *g*NC at <*N*> = ~0.1, ~0.5 and ~1.0, respectively. At <*N*> = ~0.1, the PL decay curve can be fitted by a single-exponential function with the lifetime of ~49.8 ns; At <*N*> = ~0.5, the PL decay curve can be fitted by a bi-exponential function with the long and short lifetimes of ~59.0 and ~4.4 ns, respectively; At <*N*> = ~1.0, the PL decay curve can only be fitted by a tri-exponential function with the long, medium and short lifetimes of ~48.2, ~4.9 and ~1.3 ns, respectively. The three PL decay curves are offset to each other for clarity.

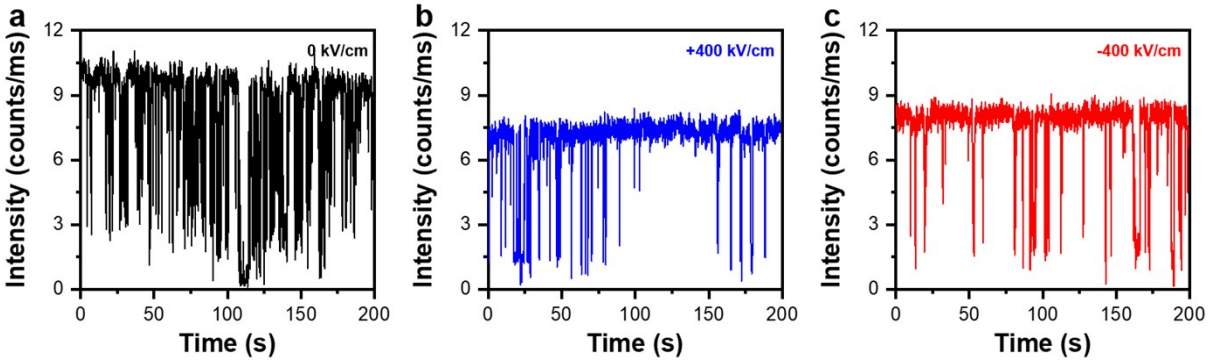

Fig. S11 (a)-(c) PL intensity time traces measured with a binning time of 10 ms for a single CdSe/CdS *g*NC excited at $< N >$ = ~0.5, showing that the PL blinking effect can be suppressed to some degree at the electric fields of ±400 kV/cm. PL decay curves measured for this single CdSe/CdS *g*NC are plotted in Figure S9c, where both the single-exciton radiative lifetime and the biexciton lifetime increase upon the application of a positive or negative electric field.

Table S1 Classification of the 47 single CdSe/CdS *g*NCs studied in the experiment into four types, according to their different electric-field induced changes in the PL spectra and PL lifetimes. Here X and XX denote single exciton and biexciton, respectively.

Types	**PL spectra**	**PL lifetimes**
Type 1 (5/47)	symmetric shift about zero field	increase for both X and XX
Type 2 (4/47)	asymmetric shift about zero field	increase for X and XX (red shift) decrease for X and XX (blue shift)
Type 3 (30/47)	no shift with the field	increase for both X and XX
Type 4 (8/47)	no shift with the field	decrease for X and increase for XX